VOL. 4, NO. 3, MAY 2009 ISSN 1819-6608
ARPN Journal of Engineering and Applied Sciences


www.arpnjournals.com

DETECTION OF HIGH-IMPEDANCE FAULTS IN TRANSMISSION LINES USING WAVELET TRANSFORM

M. Sushama, G. Tulasi Ram Das and A. Jaya Laxmi
Department of Electrical and Electronics Engineering, JNTUHCollege of Engineering, Hyderabad, India
E-Mail: m73sushama@yahoo.com

ABSTRACT

A novel approach for detection of High Impedance Faults (HIF) using wavelet transforms is presented in this work. Wavelet functions have been proposed in connection with the analysis of signals, primarily transients in a wide range of applications. The technique used here, is based on using the absolute sum value of coefficients in Multi resolution Signal Decomposition (MSD) based on the Discrete Wavelet Transform (DWT). A fault indicator and a fault criterion are then used to detect the HIF in the transmission line. The technique developed is robust to fault type, fault inception angle, fault resistance, and fault location. A new concept and methodology for HIF in transmission lines is presented. The performance of the proposed technique is tested under a variety of fault conditions on a typical 400KV transmission-line system.

Keywords: transmission lines, fault detection, high Impedance fault, wavelet transform.

1. INTRODUCTION

High-Impedance Faults (HIFs) are, in general, difficult to detect through conventional protection such as distance or over-current relays. This is principally due to relay insensitivity to the very low level fault currents and/or limitations on other relay settings imposed by HIFs. This type of fault usually occurs when a conductor touches the branches of a tree having high impedance or when a broken conductor touches the ground. In the case of an over-current relay, the low levels of current associated with HIF are below the sensitivity settings of the relay. In the case of a distance relay, which relies on an estimation of impedance to fault based on the measured voltages and currents, the accuracy of the estimation can be significantly affected by the high-impedance fault [1,2]. HIFs, albeit uncommon, must nonetheless be accurately detected and removed. This is more so in view of the fact that apart from threatening the reliability pose a risk of fires and endanger life through the possibility of electric shock.

Most conventional fault-detection techniques for HIF mainly involve processing information based on the feature extraction of post-HIF current and voltage. Several researchers in recent years have presented results aimed at detecting HIF more effectively. Hitherto, the algorithms developed include the current ratio method [3], the high-frequency method [4], the off-harmonic current method [5], the neural network and Kalman filtering method [1], [6-8]. S.J. Huang [9] has proposed an HIF detection technique [10,11] for distribution systems, which uses a Morlet wavelet transform approach [12]. However, each of these techniques improves fault detection to a certain extent, but each has its drawbacks as well. Hitherto, a few techniques (some available as commercial products) have been subjected to quite extensive testing in order to ascertain their effectiveness under different system and fault conditions.

It is well known that conventional Fourier transform-based techniques (i.e., those which rely totally on spectrum analysis of Fourier transform) do not possess the inherent time information associated with fault initiation. The wavelet transform, on the other hand, is useful in analyzing the transient phenomena associated with transmission-line faults and/or switching operations. Unlike Fourier analysis, it provides time information, has the attribute of very effectively realizing non-stationary signals comprising of low- and high-frequency components (such as those commonly encountered in power systems networks) through the use of a variable windows length of a signal [13]. The advantages (particularly in terms of increased reliability and dependability) of a wavelet transform, which possesses time and frequency information unlike the Fourier transform, particularly in the detection of HIFs, are thus apparent, and one of these techniques is the subject of this paper. It should be noted that although wavelet analysis is more complex than other signal-processing techniques, it is ideally suited for dealing with non-stationary signals such as those encountered under HIF arcing faults. This, in turn, enhances accuracy and reliability in fault detection and the features can be applied to affecting fault-location techniques [14]. This paper describes a new fault-detection technique which involves capturing the current signals generated in a transmission line under HIFs. It is shown that the technique improves the performance of HIF detection by employing the absolute sum value based on the DWT. The detection process is performed through signal decomposition, threshold of the wavelet transform coefficients, and duration time. Threshold value is determined by weighting the absolute sum value for one period in a moving window scheme and this forms the basis of sophisticated decision logic for the limitation of a trip decision.

The results presented in this paper relate to a typical 400KV Transmission line, the faulted signals of which are attained using Simulink in MATLAB 7.0.1. The simulation also includes an embodiment of a realistic nonlinear HIF model [15,16].

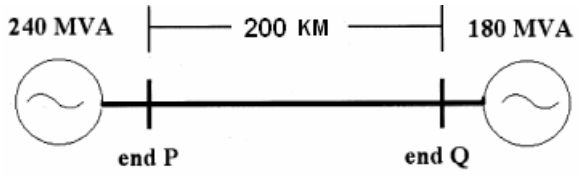

Figure-1. Transmission system (400 kV) studied.

The relay performance is then examined for HIF signals under a variety of different system and fault conditions encountered in practice.

2. DISCRETE WAVELET TRANSFORM (DWT)

Analogous to the relationship between continuous Fourier transform (FT) and Discrete Fourier Transform (DFT), the continuous wavelet transform (CWT) has a digitally implement able counterpart known as the DWT, and is defined as

$$DWT(m,k) = \frac{1}{\sqrt{a_0^m}} \sum_n x(n) g\left(\frac{k - nb_0 a_0^m}{a_0^m}\right) \quad (1)$$

Where g (n) is the mother wavelet, $x(n)$ is the input signal, and the scaling and translation parameters "a" and " b" are functions of integer parameter m. The result is geometric scaling (i.e., 1, 1/a, $1/a^2$…) and translation by 0,n, 2n…This scaling gives the DWT a logarithmic frequency coverage and this is in marked contrast to the uniform frequency coverage of, for example, the short-time Fourier transform (STFT) [13]. By simple interchange of the variables n, k, and rearrangement of the DWT (1) gives

$$DWT(m,n) = \frac{1}{\sqrt{a_0^m}} \sum_k x(k) g\left(a_0^{-m} n - b_0 k\right). \quad (2)$$

Upon closer observation of this equation, it can be noticed that there is a remarkable similarity to the convolution equation for the finite-impulse-response (FIR) digital filters, therefore

$$y(n) = \frac{1}{c} \sum_k x(k) h(n-k). \quad (3)$$

Where h (n-k) is the impulse response of the FIR filter. By comparing (2) with (3), it is evident that the impulse response of the filter in the DWT equation is

$$g\left(a_0^{-m} n - b_0 k\right). \quad (4)$$

By selecting $a_0 = {}_2$ or ($a0^{-m}$ = 1,1/2,1/4,1/8...) and b_0=1, the DWT can be implemented by using a multistage filter with the mother wavelet as the low-pass filter l (n) and its dual as the high-pass filter h (n). Also, down sampling the output of the low-pass filter l (n) by a factor of 2(↓2) effectively scales the wavelet by a factor of 2 for the next stage, thereby simplifying the process of dilation. The implementation of the DWT with a filter bank is computationally efficient. The output of the high-pass filter gives the detailed version of the high-frequency component of the signal. Also, the low-frequency component is further split to get the other details of the input signal. By using this technique, any wavelet can be implemented [13].

3. FAULT-DETECTION TECHNIQUE USING DWT

3.1 Typical waveforms through wavelet transform realization

Figure-1 shows a typical 400-kV Transmission System used in the simulation studies presented herein. It consists of a 200-km line length terminated in two sources of 240 and 180 MVA at ends P and Q, respectively; the nominal power frequency is 60 Hz. The simulation of the power system has been carried out using Simulink in Matlab 7.0.1. Within the simulation, an emulation of the nonlinear high-impedance arcing faults has also been embodied [16].

To aid the development of the fault-detection technique using the DWT, wavelet transform realization has been employed which determines a coefficient of d1 (detail one) using different mother wavelets from an actual current waveform. The mother wavelet considered is Daubechies (db) 4, biorthogonal (bior) 3.1; coiflets (coif) 4, and symlets (sym) 5. Figure-3 depicts the coefficient of d1 for different mother wavelets with the DWT realization. The behavior of the DWT for this actual fault current waveform is illustrated in Figure-2 (a)-(d) as expected. All of the coefficients of d1 increase on fault inception and there are small discernible differences in the DWT outputs for the four different mother wavelets that are considered. The performance of the DWT realization was evaluated under different fault types, fault inception angle, and fault location, and some of the results will be shown. It should be mentioned that due to a limitation of space, only the coefficient associated with "a"-earth HIF at 10 km is shown.

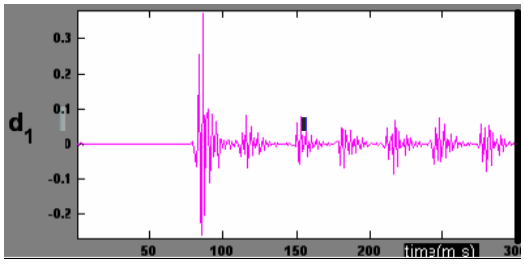

Figure-2. (a) Db4 mother wavelet.

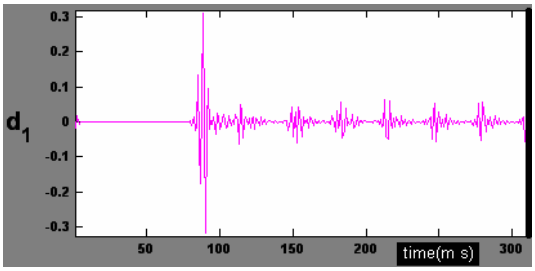

Figure-2. (b) Sym5 mother wavelet.

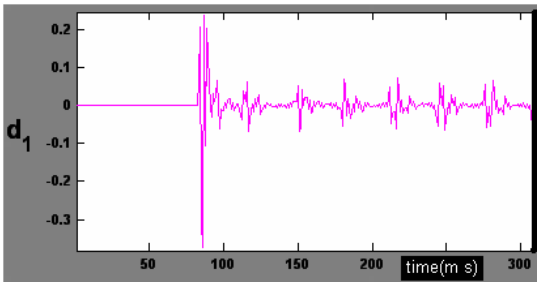

Figure-2. ((c) Bior3.1 mother wavelet.

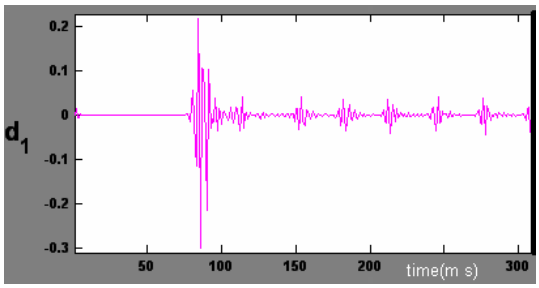

Figure-2. (d) Coif4 mother wavelet.

3.2 Selection of mother wavelet for HIF detection

As a second step in fault-detection technique, selection of the mother wavelet is essential to enhance the performance of HIF detection technique to extract the useful information rapidly. For the technique considered here, this process leads to an accurate classification between the faulted phase and the healthy phase in the first instance, thereby significantly improving the performance and speed of the HIF detection process. As mentioned in the foregoing section, the mother wavelets considered are db4, bior3.1, coif4, and sym5. For comparison of the performances attained using different mother wavelets, two conditions are compared as follows:

- A significant magnitude of d1 coefficient for detecting the fault; and
- The classification ability between the faulted phase and the healthy phase.

In order to select the most suitable mother wavelet, the maximum sum value (this is over a 1-cycle period at power frequency) of d1 coefficients based on wavelet analysis is adopted for this work. Consider, for example, the waveforms shown in Figure-3 which illustrate the maximum sum value of d1 coefficients of the three-phase current signals (as measured at the relaying point) for an "a"-earth HIF at a distance every 10km from end P in Figure-1. First of all, considering Figure-3 (a) (this is based on the db4 mother wavelet), it is clearly evident that the maximum sum value of d1 coefficients is significantly larger for the faulted "a"-phase than for the two healthy phases "b" and "c." This is also true when employing sym5 and bior3.1 mother wavelets [as evident from Figure-3 (b) and 3(c)], although the levels are somewhat smaller in the case of the former.

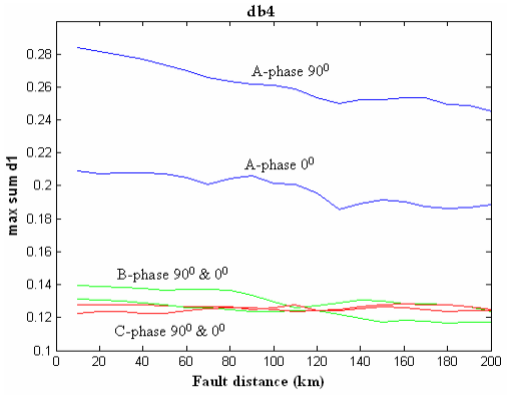

Figure-3. (a) Db4 mother wavelet.

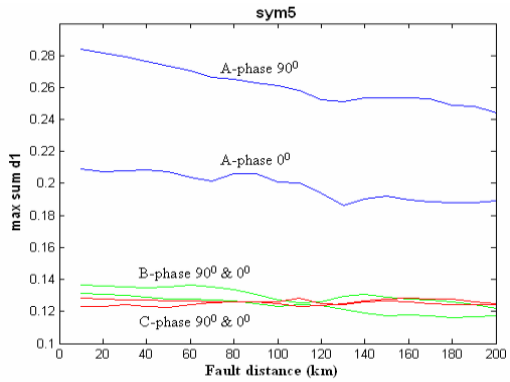

Figure-3. (b) Sym5 mother wavelet.

However, when employing the coif4 mother wavelet, although there is a discernible difference between the levels attained for the faulted "a" phase and the two healthy phases, in comparison to the previous three mother wavelets considered, they are significantly lower. Also, equally important is that the difference s in magnitudes between the faulted and healthy phases in the case of coif4 is much smaller than the corresponding other types of mother wavelets as apparent from the graphs shown in Figure-4, and this is true for all fault positions. Thus, with regard to the selection of the mother wavelet, the simple criterion adopted herein is based on the magnitudes of the summated coefficients d1 and the differences in magnitudes between the faulted and healthy phases. In this respect, after a series of studies employing the foregoing d1 coefficients distribution approach, the db4 and sym5 are appropriate for detection of HIF in transmission line. The db4 mother wavelet is chosen for this study.

3.3 Fault-detection algorithm

Figure-4 shows the fault-detection procedure of the proposed technique, where FI is a counter that signifies the sample number (and, therefore, the time period) for which useful information through DWT realization under HIF persists. Is the sum value of the detailed output (d1 component) for a 1-cycle period and is represented as an

absolute value, fault criterion (FC) is the signal magnitude threshold as the lower limit of that is used to detect the HIF, and is the sample number that signifies the duration time for which a transient event (such as HIF) has to persist continuously. This is to discriminate between HIF and non-fault transient events such as capacitor and line switching, arc furnace loads, etc. As can be seen, when is greater than or equal to FC, the value of FI is incremented and as soon as it attains the level, this indicates an internal fault and a trip signal is initiated. As shown in Figure-4, the absolute sum value is based on summating the d1 coefficients over a 1-cycle period and the sampling rate employed is 3840 Hz (i.e.64samples/cycle at 60 Hz). The summated values associated the three phases are compared with a preset threshold level FC. The whole process is based on a moving window approach where the 1-cycle window is moved continuously by one sample. It is apparent from the foregoing decision logic that the criteria for the protection relay to initiate a trip signal is such that must stay above the threshold level FC continuously for samples (after fault inception). In this respect, an extensive series of studies has revealed that in order to maintain relay stability for external faults (i.e., faults behind bus bar P and beyond busbar Q in Figure-1) and also restrain under no-fault conditions, the optimal settings for FC and D are 5 and 192, respectively. The setting values of these thresholds are dependent on the system environments. Note that the latter corresponds to a three-cycle period at power frequency.

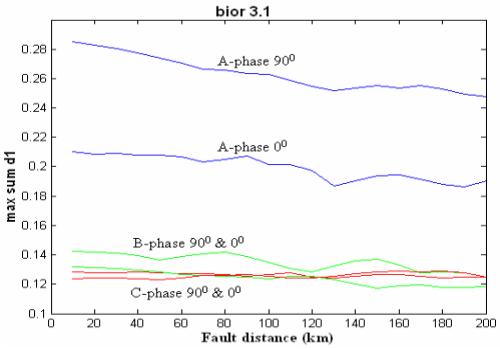

Figure-3. ((c) Bior3.1 mother wavelet**.**

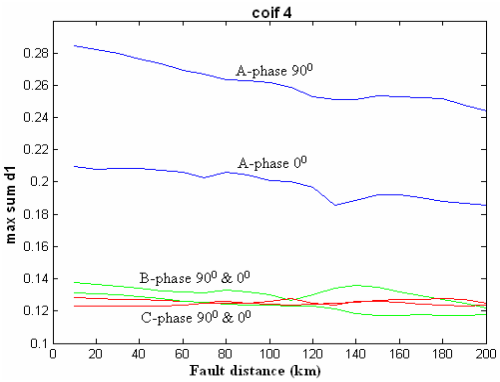

Figure-3. (d) Coif4 mother wavelet.

4. SIMULATION RESULTS

In this section, some typical results illustrate the performance of the protection technique being developed. It should be noted that although not shown herein, responses/ limitations due to CTs, relay hardware (such as current interface module comprising anti-aliasing filters and analog to digital converters), etc. have been taken into account in the simulation so that the relay performance attained pertains closely to that expected in reality.

4.1 Single-phase-earth fault

Figure-5 depicts the absolute sum value of d1 associated with the three-phase currents (measured at end P of the system shown in Figure-1) using the db4 mother wavelet; the graphs shown in Figure- 5(a) and 5(b) are for an "a"-phase-earth HIF, as a function of fault distance and are for fault inception angles of 90^0 and 0^0, respectively. As expected, the magnitudes of the faulted "a" phase is much higher than the healthy phases and this is true for both fault inception angles considered.

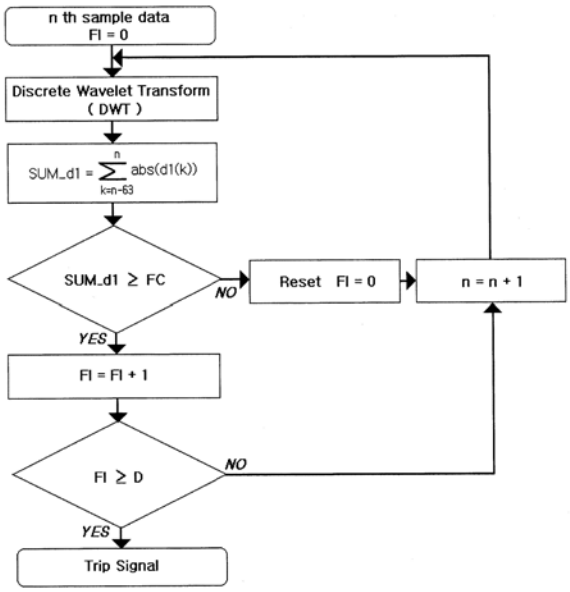

Figure-4. Flow chart- fault-detection technique.

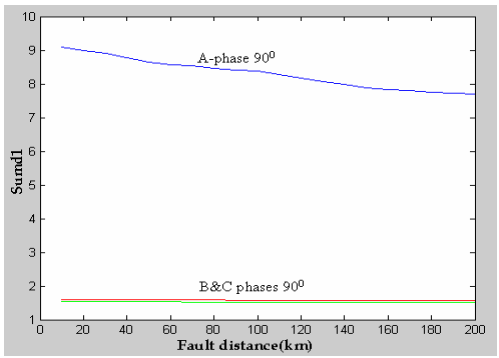

Figure-5. (a) ARC A-G fault (fault inception angle 90^0).

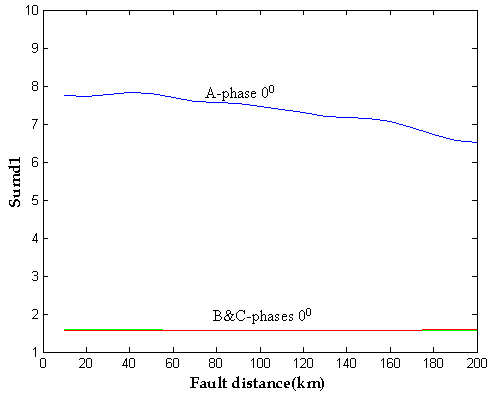

Figure-5. (b) ARC A-G fault (fault inception angle 0^0).

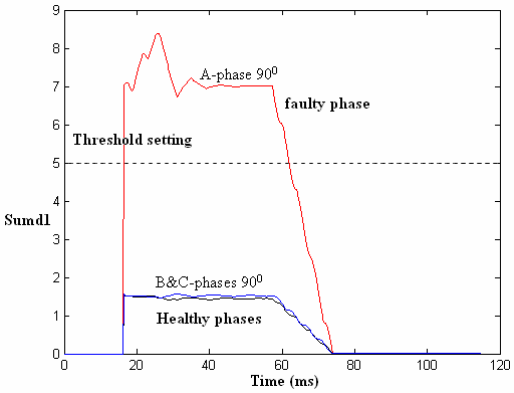

Figure-6. (a) ARC A-G fault at 100km (inception angle 90^0).

Also important, although the magnitudes reduce in size as the fault moves away from end P, the very significant difference between the faulted and healthy phases is retained for an appreciable time period. It should be mentioned that in all HIF cases, the fault impedance has been represented by a realistic nonlinear arc model, but for reference purposes only, this can be considered as approximately equivalent to about 300Ω. Figure-6 shows the behavior of absolute sum value of d1 for one particular fault position (i.e. 100 km from end P, as a function of time, the graphs also depict the moving-window regime adopted). It is apparent that for both fault inception angles considered, the faulted "a" phase stays above the set threshold level (FC=5) for more than three cycles; this corresponds to a sample number of approximately 192 and is well above the set level of D=192. The protective relay will thus initiate a trip signal. For comparison purposes, the healthy phase currents "b" and "c" are also shown and, as expected their magnitudes are well below the threshold level FC=5.

4.2 Double-phase-earth fault

Figure-7 typifies the variations in the absolute sum values of the coefficients d1 for a double-phase-earth HIF fault. The graphs shown are for two fault inception angles; one near voltage maximum of the "a"-phase [Figure-7 (a)] and the other is in relation to voltage zero of

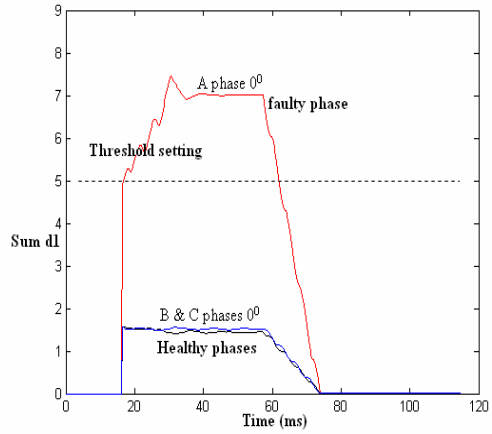

Figure-6 (b). ARC A-G fault at 100km (inception angle 0^0).

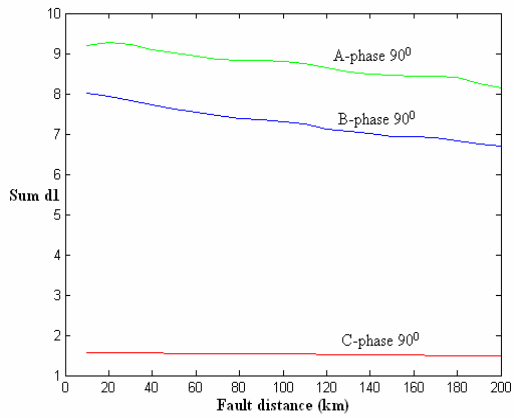

Figure-7 (a). ARC A-B-G fault (fault inception angle 90^0).

the "a"-phase [Figure-7 (b)]. Here again, there is a large difference in magnitudes between the faulted phases and the healthy phase and, as expected, both of the faulted phases ("a" and "b" involved in the fault) attain high levels.

When considering the dynamic behavior of the absolute sum value as a function of time, for one particular fault position (which is 100 km from end P in Figure-1),

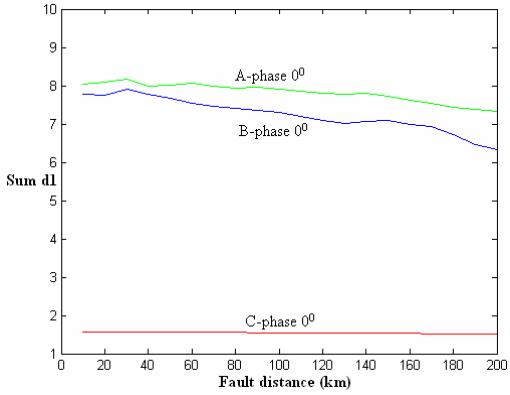

Figure-7 (b). ARC A-B-G fault (fault inception angle 0^0).

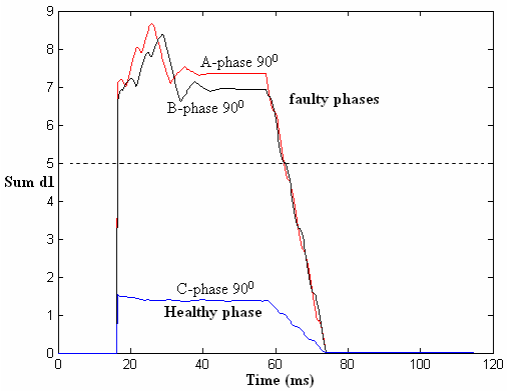

Figure-8 (a). ARC A-B-G fault at 100km (inception angle 90^0).

Figure-8 portrays characteristics which are very much in line with what is expected (i.e., both the faulted phases "a" and "b" stay well above the set level FC=5.) for an appreciable time after fault inception and the healthy phase stays well below the threshold throughout the period of interest.

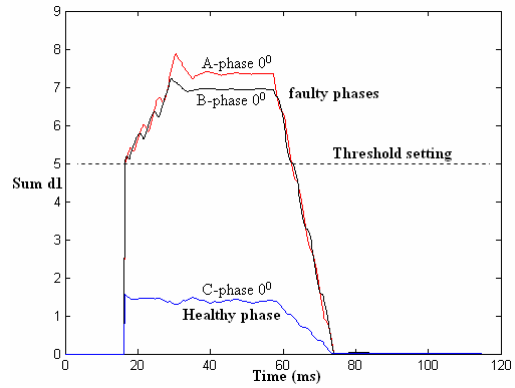

Figure-8 (b). ARC A-B-G fault at 100km (inception angle 0^0).

4.3 Non-fault transient events

In the development of any new fault-detection technique, such as the type described in this paper, it is important to ensure that it is secure under non-fault events such as capacitor and line switching, arc furnace loads, etc. In this respect, it should be noted that for this fault detector, the parameter 'D' (comprising of 192 samples) within the decision logic plays a crucial role in maintaining the fault detector's security.

5. CONCLUSIONS

A novel technique for transmission -line fault detection under high-impedance faults using the discrete wavelet transform is presented for which a near optimal mother wavelet (suitable for a vast majority of different samples and fault conditions) has been selected after an extensive series of studies.

The DWT-based technique presented herein has a number of distinct advantages over other traditional HIF detection techniques. It is robust to a variation in different system and fault conditions and is predominantly dependent upon the nonlinear behavior of the HIF and has the ability to discriminate clearly between internal faults and external faults. It has the inherent attribute of distinguishing between the faulted phase(s) and healthy phase(s) and this is a significant advantage for transmission systems in which single-pole tripping is employed, and which therefore requires phase selection. The technique developed is based on current signals only and, therefore, requires the use of current transformers (CT's) only.

REFERENCES

[1] F. Sultan, G. W. Swift, and D. J. Fedirchuk. 1992. Detection of high impedance arcing faults using a multi-layer perceptron. IEEE Trans. Power Delivery. 7: 1871-1877, Oct.

[2] B. D. Russel, C. L. Benner, and A. V. Mamishev. 1996. Analysis of high impedance fault using fractal techniques. IEEE Trans. Power Syst. 11: 435-440, Feb.

[3] D. I. Jeerings and J. R. Linders. 1991. A practical protective relay for down-conductor faults," IEEE Trans. Power Delivery. 6: 565-574, Apr.

[4] A. Girgis, W. Chang, and E. B. Makram. 1990. Analysis of high -impedance fault generated signals using a Kalman filtering approach. IEEE Trans. Power Delivery. 5: 1714-1722, Oct.

[5] S. Ebron, S. L. Lubkeman. And M. White. 1990. A n eural network approach to the detection of incipient faults on power distribution feeders. IEEETrans. Power Delivery. 5: 905-912, Apr.

[6] S. J. Huang and C. T. Hsieh. 1999. High impedance fault detection utilizing a Morletwavelet transform approach. IEEE Trans. Power Delivery. 14: 1401-1410, Oct.

[7] E. Emanuel and E. M.Gulachenski. 1990. High impedance fault arcing on sandy soil in 15 kV distribution feeders: Contributions to the evaluation of the low frequency spectrum. IEEE Trans. Power Delivery. 5: 676-686, Apr.

[8] D. C. T.Wai and X. Yibin. 1998. A novel technique for high impedance fault identification, IEEE Trans. Power Delivery. 13: 738-744, July.

[9] O. Chaari, M. Meunier. And F. Brouaye. 1996. Wavelets: A new tool for the resonant grounded power distribution systems relaying. IEEE Trans. Power Delivery. 11: 1301-1308, July.

[10]F. H. Magnago and A. Abur. 1998. Fault location using wavelets. IEEETrans. Power Delivery. 13: 1475-1480, Oct.

[11]V. L. Buchholz, M. Nagpal, J. B. Neilson. And W. Zarecki. 1996. High impedance fault detection device tester. IEEE Trans. Power Delivery. 11: 184-190, Jan.

[12]O. Chaari, M. Meunier, and F. Brouaye. 1996. Wavelets: A new tool for the resonant grounded power distribution systems relaying. IEEE Trans. Power Delivery. 11: 1301-1308, July.

[13]G. Strang and T. Q. Nguyen. 19960. Wavelets and Filter Banks. Cambridge, MA: Wellesley-Cambridge.

[14]F. H. Magnago and A. Abur. 1998. Fault location using wavelets. IEEE Trans. Power Delivery. 13: 1475-1480, Oct.

[15]V. L. Buchholz, M. Nagpal, J. B. Neilson, and W. Zarecki. 1996. High impedance fault detection device tester. IEEE Trans. Power Delivery. 11: 184-190, Jan.

[16]T. Johns, R. K. Aggarwal, and Y. H. Song. 1994. Improved techniques for modeling fault arcs on faulted EHV transmission systems. Proc. Inst. Elect. Eng. Gener. Transm. Distr. 144(2): 148-154.